Two-Dimensional NMR Studies of Squash Family Inhibitors. Sequence-Specific Proton Assignments and Secondary Structure of Reactive-Site Hydrolyzed *Cucurbita maxima* Trypsin Inhibitor III†

Ramaswamy Krishnamoorthi,* YuXi Gong,‡ and Chan-Lan Sun Lin

Department of Biochemistry, Kansas State University, Manhattan, Kansas 66506

David VanderVelde

Department of Medicinal Chemistry, University of Kansas, Lawrence, Kansas 66045

Received March 28, 1991; Revised Manuscript Received September 16, 1991

ABSTRACT: The solution structure of reactive-site hydrolyzed *Cucurbita maxima* trypsin inhibitor III (CMTI-III*) was investigated by two-dimensional proton nuclear magnetic resonance (2D NMR) spectroscopy. CMTI-III*, prepared by reacting CMTI-III with trypsin which cleaved the Arg5–Ile6 peptide bond, had the two fragments held together by a disulfide linkage. Sequence-specific ^{1}H NMR resonance assignments were made for all the 29 amino acid residues of the protein. The secondary structure of CMTI-III*, as deduced from NOESY cross peaks and identification of slowly exchanging hydrogens, contains two turns (residues 8–12 and 24–27), a 3_{10}-helix (residues 13–16), and a triple-stranded β-sheet (residues 8–10, 29–27, and 21–25). This secondary structure is similar to that of CMTI-I [Holak, T. A., Gondol, D., Otlewski, J., & Wilusz, T. (1989) *J. Mol. Biol. 210*, 635–648], which has a Glu instead of a Lys at position 9. Sequential proton assignments were also made for the virgin inhibitor, CMTI-III, at pH 4.71, 30 °C. Comparison of backbone hydrogen chemical shifts of CMTI-III and CMTI-III* revealed significant changes for residues located far away from the reactive-site region as well as for those located near it, indicating tertiary structural changes that are transmitted through most of the 29 residues of the inhibitor protein. Many of these residues are functionally important in that they make contact with atoms of the enzyme in the trypsin–inhibitor complex, as revealed by X-ray crystallography [Bode, W., Greyling, H. J., Huber, R., Otlewski, J., & Wilusz, T. (1989) *FEBS Lett. 242*, 285–292]. Furthermore, comparison of backbone hydrogen chemical shifts of CMTI-I [Holak, T. A., Gondol, D., Otlewski, J., & Wilusz, T. (1989) *J. Mol. Biol. 210*, 635–648] and CMTI-III, on the other hand, indicated changes for fewer residues located near the site of substitution (Glu9 in CMTI-I and Lys9 in CMTI-III) as well as away in the C-terminal region; residues that form the secondary structural elements showed chemical shift perturbations, whereas those in an extended conformation did not. These chemical shift changes were relatively small (<0.15 ppm) compared to changes that occurred upon hydrolysis of the reactive-site peptide bond between Arg5 and Ile6 in CMTI-III (up to 0.64 ppm).

The squash family of serine proteinase inhibitors includes small proteins of 29–32 amino acid residues, including three disulfide bridges (Wieczorek et al., 1985; Otlewski, 1990). These proteins are inhibitors of biologically important molecules such as trypsin, activated Hageman factor (Hojima et al., 1982), human leukocyte elastase, and cathepsin G (McWherter et al., 1989) and hence are important candidates for developing drugs for cardiovascular diseases and inflammatory cell proteolysis based on their structural information. Furthermore, the ability to chemically synthesize both naturally occurring *Cucurbita maxima* trypsin inhibitor (CMTI)[1] and its variants has opened up a powerful avenue for establishing structure–function relationships for this class of proteins (Kupryszewski et al., 1986; McWherter et al., 1989). The X-ray crystallographic structure of CMTI-I complexed with β-trypsin was obtained recently (Bode et al., 1989). The solution structure of CMTI-I at low pH (4.7–5.3) obtained by two-dimensional nuclear magnetic resonance (2D NMR) spectroscopy and a combination of distance-geometry algorithm and dynamical simulated annealing (Holak et al., 1989a,b) agrees with that obtained by X-ray crystallography. The binding site of CMTI-I, including the geometry of the Arg5–Ile6 reactive-site peptide bond, is similar to those observed for other serine proteinase inhibitors. The inhibitor protein mainly possesses only turns. Residues Arg1–Leu7, Glu9, and His25–Gly29 make 138 intermolecular contacts with trypsin in the enzyme–inhibitor complex (Bode et al., 1989). Reaction of proteinaceous inhibitors with trypsin results in the formation of modified inhibitors, in which the reactive-site peptide bond is hydrolyzed (Laskowski & Kato, 1980). In the case of CMTI's, the fragments are still held

† This study was supported by grants from the American Heart Association, Kansas Affiliate, and the Wesley Foundation, Wichita, KS (to R.K.).

* To whom correspondence should be addressed.

‡ Permanent address: Testing Center, Hubei Academy of Agricultural Science, Wuhan, China.

[1] Abbreviations: CMTI, *Cucurbita maxima* trypsin inhibitor; 2D, two dimensional; NMR, nuclear magnetic resonance; NOE, nuclear Overhauser effect; TOCSY, total correlated spectroscopy; DQF-COSY, double-quantum filtered correlated spectroscopy; NOESY, two-dimensional NOE spectroscopy; CMTI-I*, reactive-site hydrolyzed CMTI-I; CMTI-III*, reactive-site hydrolyzed CMTI-III; ppm, parts per million; EETI-II, *Ecballium elaterium* trypsin inhibitor II.

0006-2960/92/0431-898$03.00/0

together by means of a connecting disulfide bridge. An interesting property of the reactive-site modified CMTI-I and CMTI-III (CMTI-I* and CMTI-III*, respectively) is that while both of them inhibit trypsin, they are not able to inhibit activated Hageman factor (factor XII_a; Hojima et al., 1982; Krishnamoorthi et al., 1990). It is, therefore, of interest to identify structural changes that cause the loss of the inhibitor's activity toward factor XII_a. That knowledge may be useful in the development of inhibitors of improved or different functions.

Herein we report on the solution structure of reactive-site hydrolyzed CMTI-III (CMTI-III*) as obtained by the application of 2D NMR techniques and show that while the secondary structure is preserved in solution, tertiary structural changes occur throughout the protein molecule as a result of the Arg5–Ile6 peptide bond cleavage. Furthermore, comparison of backbone hydrogen chemical shifts of the virgin inhibitors, CMTI-III and its Lys9 → Glu variant CMTI-I, indicates that the residues making the secondary structure are perturbed, whereas those in an extended conformation are not.

Materials and Methods

Proteins. CMTI-III and CMTI-III* were isolated from pumpkin seeds by means of trypsin affinity chromatography, followed by high-performance liquid chromatography (HPLC; Krishnamoorthi et al., 1990). Reaction of CMTI-III with trypsin produced CMTI-III*. CMTI-III* was found to be quite stable for months, as judged by HPLC results. NMR samples (4–15 mM) were prepared in both 90% ^1H_2O/10% ^2H_2O and 99.9% ^2H_2O by dissolving lyophilized protein in 400–500 μL of the solvent that contained 0.2 M KCl. The pH's of the samples were adjusted with 0.2 M ^2HCl and/or 0.2 M NaO^2H by using an Ingold microcombination glass electrode and a Fisher pH meter (model 815 MP).

NMR Spectroscopy. One- and two-dimensional NMR experiments were carried out with a Bruker AM 500 instrument operating at 500.14 MHz for ^1H. Data were processed on a Silicon Graphics workstation, using the software FELIX (Hare Research Inc., Woodinville, WA). The following 2D NMR experiments were performed: double-quantum filtered COSY (DQF-COSY; Piantini et al., 1982; Rance et al., 1983); total correlated spectroscopy (TOCSY; Braunschweiler & Ernst, 1983) with an MLEV spin lock (Bax & Davis, 1985); phase-sensitive nuclear Overhauser effect spectroscopy (NOESY; Anil Kumar et al., 1980). In the case of TOCSY experiments, two sets of data were acquired with mixing times of 50 and 70 ms. For NOESY experiments, the mixing time was varied from 200 to 700 ms. All data were collected by using time-proportional phase incrementation (TPPI; Marion & Wüthrich, 1983). Typically, 2D data were acquired by collecting 400–512 blocks of 2048 data points each. Before processing the data were zero-filled once in the F_1 dimension. Chemical shifts were referenced with respect to the water peak, which was assigned a value of 4.71 ppm at 30 °C. For the purpose of locating $C_\alpha H$ peaks that occurred close to the water peak (those of Lys residues), TOCSY and NOESY data sets were acquired at 10 and 45 °C. Exchange of solvent-labile backbone NH's with deuterated water was followed by collecting either 1D NMR spectra at a series of time intervals of 10 min or less or by collecting a series of DQF-COSY data every 2 h or less.

Results

Identification of Spin Systems and Sequential Assignments. CMTI-III* has one each of Pro, Ile, Met, His, Tyr, Ala, and

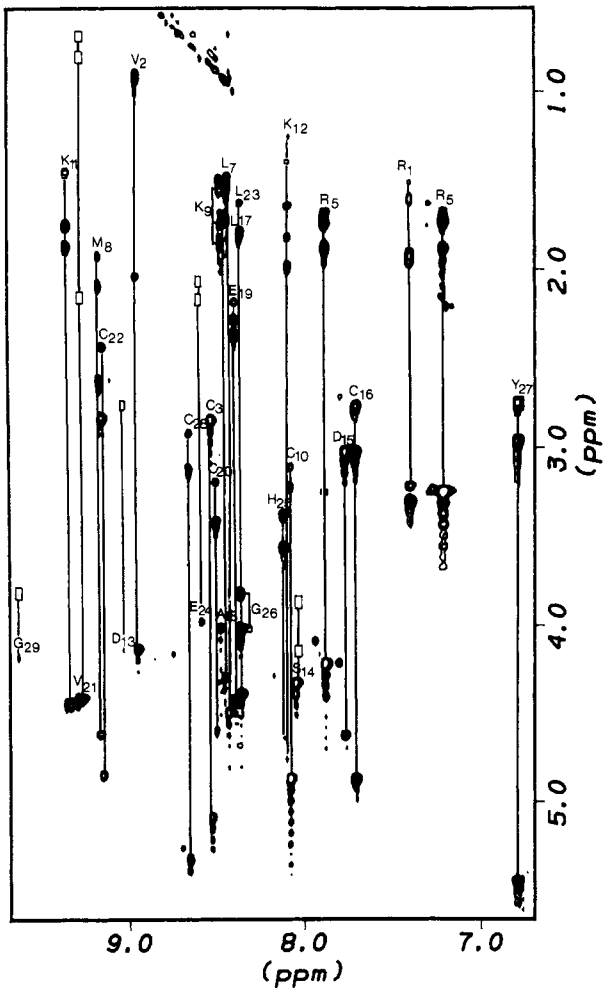

FIGURE 1: 500-MHz TOCSY map of CMTI-III* in 90% H_2O, pH 4.71, 30 °C obtained with a mixing time of 70 ms. Cross peaks that were observed at lower contour levels are identified by square boxes. Assignments indicated were obtained by the sequential assignment procedure (Wüthrich, 1986).

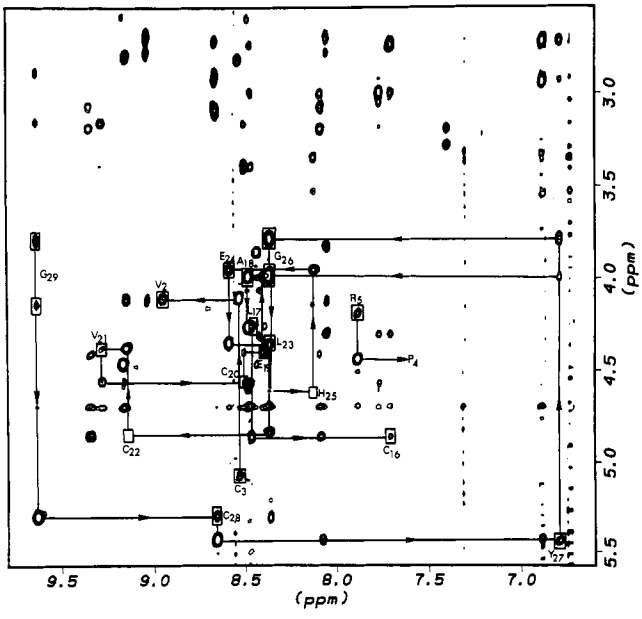

FIGURE 2: NOESY contour map of CMTI-III* in 90% H_2O, pH 4.71, 30 °C. Sequential $d_{\alpha N}(i,i+1)$ connectivities are shown for residues Gly29 → Cys16 and Arg5 → P4. The square boxes indicate either the intraresidue $d_{\alpha N}$ COSY cross peaks observed or the positions where cross peaks are observed in the DQF-COSY map.

Table I: Chemical Shifts of the Assigned ^{1}H NMR Resonances of CMTI-III and CMTI-III* at pH 4.71, 30 °C[a]

	NH		C_αH		C_βH		C_γH		others	
residue	CMTI-III	CMTI-III*	CMTI-III	CMTI-III*	CMTI-III	CMTI-III*	CMTI-III	CMTI-III*	CMTI-III	CMTI-III*
Arg1			4.07	4.12	1.58, 1.87	2.04	1.42	1.92	3.30 7.31	3.28, 3.21, 7.38
Val2	9.04	8.93	4.05	4.10	2.03	2.04	0.88, 0.95	0.92, 0.95		
Cys3	8.52	8.55	5.21	5.07	2.67, 2.82	2.83				
Pro4			4.45	4.43	2.36	2.26, 2.36	2.03	1.98, 2.05	3.65, 3.89	3.70, 3.75
Arg5	8.54	7.90	4.33	4.18	1.73, 1.95	1.87		1.68	3.27 7.16	3.23 7.21
Ile6	7.40		4.13	3.87	1.68	1.97	1.05, 1.36	1.01, 1.21, 1.48	0.86	0.93
Leu7	8.69	8.44	4.37	4.47	1.53, 1.75	1.51		1.46	0.75, 0.82	0.63, 0.68
Met8	9.11	9.18	4.49	4.60	2.02, 1.86	1.90, 2.08	2.49, 2.65	2.62		
Lys9	8.55	8.49	4.45	4.69	1.60, 1.66	1.85		1.70, 1.75	1.74 2.98	1.38, 1.54, 3.04
Cys10	8.08	8.08		4.84	3.10, 3.21	3.10, 3.22				
Lys11	9.36	9.36	4.34	4.43	1.76	1.76, 1.87	1.45	1.44	1.88 2.99	1.67, 2.98
Lys12	8.10	8.07		4.75	1.65, 1.99	1.97, 1.99	1.25, 1.39	1.66, 1.83	1.83 2.97	1.26, 1.40, 2.99
Asp13	9.03	9.05	4.06	4.14	2.73, 2.81	2.71, 2.79				
Ser14	8.04	8.07	4.26	4.31	3.87, 4.19	3.83, 4.15				
Asp15	7.75	7.77	4.49	4.62	3.01	3.00, 3.18				
Cys16	7.66	7.72	4.91	4.85	2.77, 3.09	2.76, 3.02				
Leu17	8.63	8.48	4.21	4.28	1.51, 1.71	1.55, 1.70		1.70	0.84, 0.93	0.93, 0.95
Ala18	8.51	8.48	3.92	3.99	1.48	1.48				
Glu19	8.44	8.39	4.41	4.40	2.19, 2.27	2.17, 2.28	2.36, 2.42	2.35		
Cys20	8.64	8.50	4.48	4.58	3.40, 3.23	3.16, 3.42				
Val21	9.36	9.28	4.33	4.38	2.15	2.17	0.74, 0.84	0.71, 0.82		
Cys22	9.23	9.17	4.91	4.86	2.42, 2.84	2.44, 2.84				
Leu23	8.26	8.36	4.36	4.37	1.81, 1.99	1.63, 1.78	1.71	1.73	0.82, 0.94	0.78, 0.88
Glu24	8.59	8.57	3.95	3.97	1.92, 2.01	1.88, 1.98	2.09, 2.16	2.07, 2.12		
His25	8.21	8.11		4.64	3.47, 3.56	3.37, 3.56			7.27, 8.48	7.81, 8.55
Gly26	8.36	8.37	3.71, 3.94	3.78, 4.00						
Tyr27	6.87	6.82	5.31	5.43	2.67, 3.07	2.73, 2.94			6.70, 6.87	6.73, 6.88
Cys28	8.48	8.68	5.29	5.32	2.93, 3.16	2.92, 3.08				
Gly29	9.73	9.63	3.72, 4.10	3.82, 4.15						

[a] Chemical shifts are accurate to ±0.025 ppm.

Ser, two each of Glu, Asp, Arg, Gly, and Val, three each of Leu and Lys, and six half-cysteine residues. Identification of spin systems was achieved from a combined analysis of DQF-COSY and TOCSY maps (Wüthrich, 1986). Four different regions were analyzed: in region A [3.5–4.5 ppm (F_2); 3.5–4.5 ppm (F_1)], the spin systems of Gly (AX) and Ser (AMX) were identified. In region B [2.5–4.0 ppm (F_2); 4.0–5.5 ppm (F_1), the AMX spin systems of Cys, Asp, His, and Tyr were assigned. In region C [(1.0–3.0 ppm (F_2); 3.5–5.0 ppm (F_1)], Glu, Ala, Arg, Met, and Lys spin systems were assigned. In region D [0.5–2.5 ppm (F_2); 3.5–4.5 ppm (F_1)], spin systems of Val, Ile, and Leu (A_3B_3MX, A_3MPTB_3X, A_3B_3MPTX) were identified. The last one to be identified was Pro (A_2T_2MPX). These assignments are indicated in Figure 1, which displays a portion of TOCSY contour map of CMTI-III* dissolved in 90% ^1H_2O/10% ^2H_2O. With several unique residues having been identified, it was relatively easy to carry out sequential assignments (Wüthrich et al., 1982; Wüthrich, 1986) in different short and long stretches in the finger print region [6.5–10.0 ppm (F_2); 0.5–5.5 ppm (F_1)]: starting with Gly29, the assignment proceeded via the $d_{N\alpha}$ connectivities to Cys16. Starting from Ser14, assignments were extended in the directions of both the C- and N-terminals to Asp15 and Asp13; similarly, starting with Met8, assignments were effected up to Lys12 in the C-terminal direction and to Ile6 in the N-terminal direction. These stretches were chosen because of difficulties in locating NOESY cross peaks from the following $C_\alpha H_i$–$N_{(i+1)}H$ connectivities: Lys12–Asp13 and Asp15–Cys16. Because the Arg5–Ile6 peptide bond was hydrolyzed in the modified form of the inhibitor, there was no $d_{N\alpha}(i,i+1)$ NOE cross peak to be observed between Arg5 and Ile6. A strong $d_{N\alpha}$(Arg5–Pro4) was used to assign Arg5. Similarly, a strong $d_{\alpha\delta}$(Cys3–Pro4) cross peak at 5.07 and 3.75 ppm led to the assignment of Cys3, and a strong $d_{N\alpha}$(Cys3–Val2) cross peak at 8.55 and 4.10 ppm resulted in the assignments of Val2 and Cys3. These assignments are shown in NOESY maps of CMTI-III* in 90% ^1H_2O/10% ^2H_2O (Figures 2 and 3) obtained with a mixing time of 200 ms. The sequence-specific proton assignments are listed in Table I.

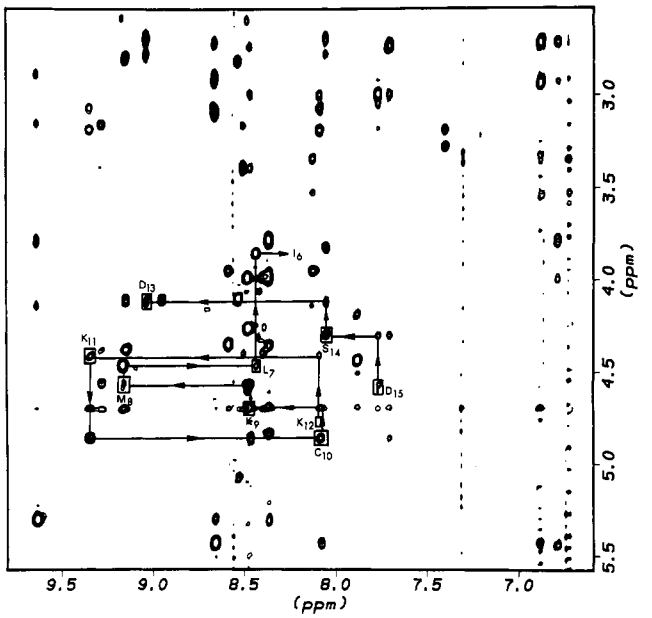

FIGURE 3: NOESY contour map of CMTI-III* in 90% H_2O, pH 4.71, 30 °C. Sequential $d_{\alpha N}(i,i+1)$ connectivities are shown for residues Asp15 → Ile16. The square boxes represent either the intraresidue $d_{\alpha N}$ COSY cross peaks observed or the positions where cross peaks are observed in the DQF-COSY map.

Identification of Secondary Structural Elements. Figure 4 displays the amide region of the NOESY map of CMTI-III* containing d_{NN} connectivities. Cross peaks are observed between residues Cys10 and Lys11, and Gly 26 and Tyr27, indicating the presence of turns in this region (Billeter et al.,

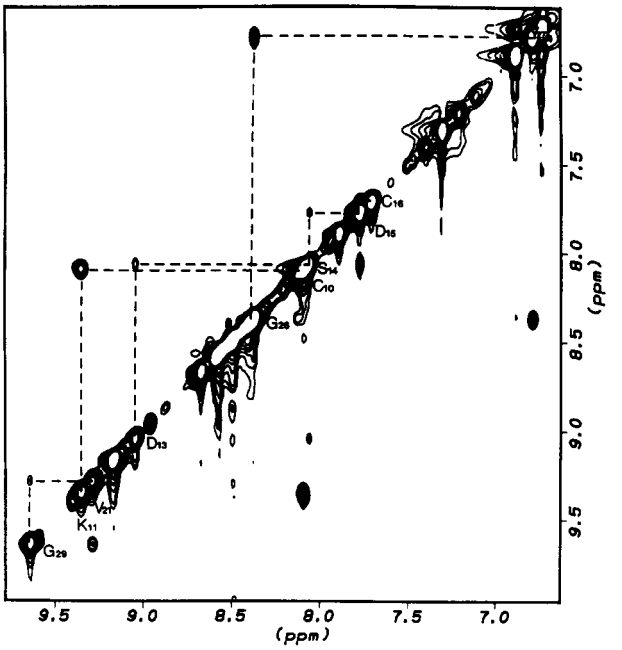

FIGURE 4: NOESY contour map of CMTI-III* in 90% H_2O, pH 4.71, 30 °C. The $d_{NN}(i,i+1)$ connectivities are indicated. Cross peaks in this region are characteristic of turns and helices (see text).

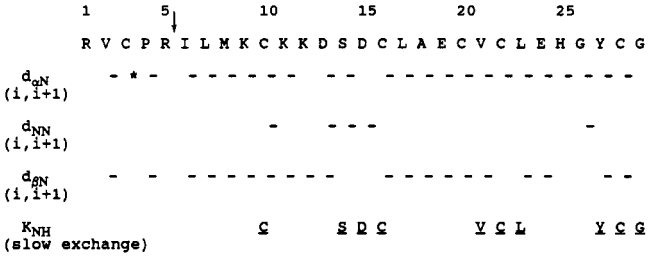

FIGURE 5: Summary of interresidue NOE connectivities observed for CMTI-III* with a mixing time of 200 ms. Also identified are backbone peptide NH's that are hydrogen-bonded, as indicated by slower deuterium exchange kinetics. The asterisk (*) indicates that Pro4 has no backbone NH.

1982; Wüthrich, 1986; Bax, 1989). The cross peak assigned to Cys10–Lys11 connectivity could also be assigned to a Lys11–Lys12 interaction because of degeneracy of the peptide NH's of Cys10 and Lys12 at 8.08 ppm. The degeneracy could not be removed at either 10 or 45 °C. Similar $d_{NN}(i,i+1)$ cross peaks are also observed between residues Asp13 and Ser14, Ser14 and Asp15, and Asp15 and Cys16. The d_{NN} Asp15–Cys16 cross peak occurring close to the diagonal is confirmed by its increased intensity and better definition at a higher NOE mixing time of 700 ms (data not shown). In addition, weak $d_{N\alpha}$ Asp13–Asp15, Cys16–Asp13, and Cys16–Ser14 are also observed. However, we do not observe any $d_{NN}(i,i+2)$ or $d_{NN}(i,i+3)$ connectivities for this segment, indicating the absence of a regular α-helix. The observed cross-peak patterns for the four residues 13–16 are consistent with them forming a 3_{10}-helix. A d_{NN} Val21–Gly29 cross peak also occurs, indicating the proximity of these two residues. These d_{NN} connectivities and also other interresidue connectivities, $d_{\alpha N}(i,i+1)$ and $d_{\beta N}(i,i+1)$, are summarized in Figure 5. The 200-ms NOESY contour map shows the presence of many other cross peaks: These connectivities, viz., $d_{\alpha N}(i,j)$, $d_{\alpha\alpha}(i,j)$, $d_{\alpha\beta}(i,j)$, and $d_{\beta\beta}(i,j)$, are summarized (Supplementary Material) and presented along with the above-mentioned NOE connectivities in Figure 6. The upper diagonal part presents backbone–backbone interactions, whereas the lower diagonal

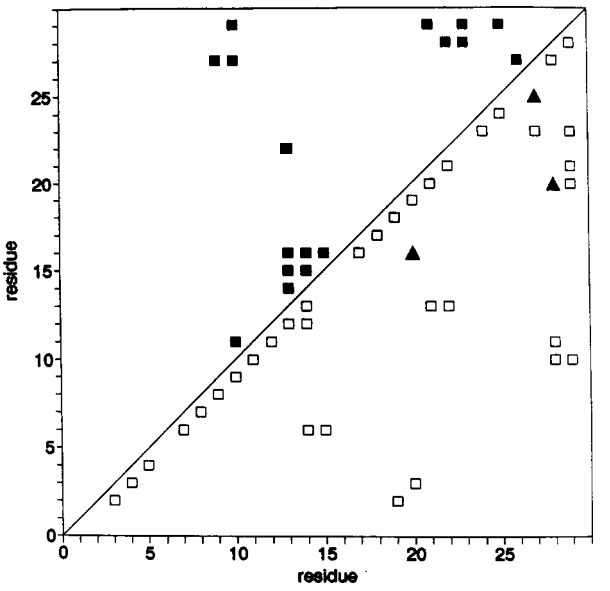

FIGURE 6: Diagonal plot of short-range NOE cross peaks obtained with a NOESY mixing time of 200 ms for CMTI-III* at pH 4.71, 30 °C. Observed backbone–backbone interactions (filled squares) are represented above the diagonal, whereas backbone–side chain (open squares) and side chain–side chain (filled triangles) interactions are represented below the diagonal.

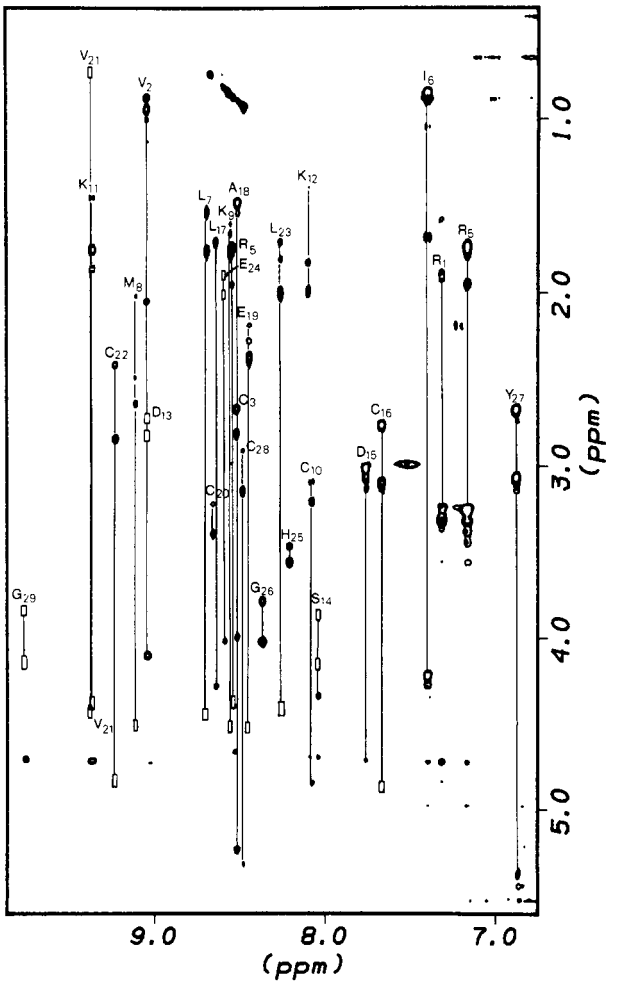

FIGURE 7: TOCSY map of CMTI-III in 90% H_2O, pH 4.71, 30 °C. Square boxes indicate cross peaks that are either observed at lower contour levels or positions corresponding to cross peaks observed in DQF-COSY and NOESY maps. Assignments indicated were obtained by the sequential assignment procedure (Wüthrich, 1986).

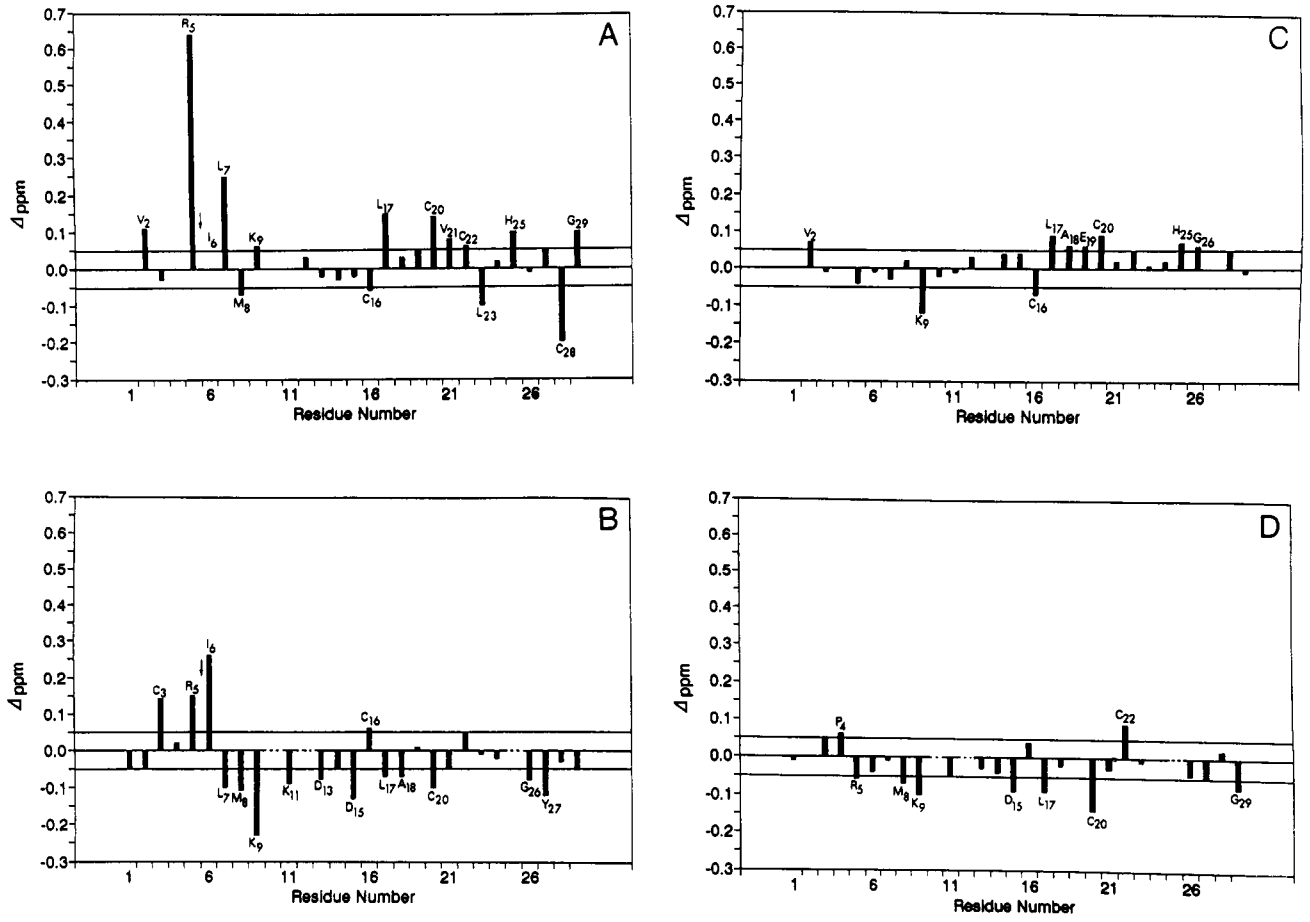

FIGURE 8: Backbone hydrogen chemical shift differences between virgin (CMTI-III) and modified (CMTI-III*) squash inhibitor, and between CMTI-III and CMTI-I; CMTI-III has a Lys in position 9, whereas CMTI-I has a Glu (Wieczorek et al., 1985). Chemical shift data for CMTI-I are taken from the work of Holak et al. (1989a). (A) NH chemical shift difference (CMTI-III–CMTI-III*); (B) $C_\alpha H$ chemical shift difference (CMTI-III–CMTI-III*); (C) NH chemical shift difference (CMTI-III–CMTI-I); (D) $C_\alpha H$ chemical shift difference (CMTI-III–CMTI-I). The arrow indicates the Arg5–Ile6 peptide bond which is cleaved in CMTI-III*. The chemical shift of the NH of Ile6 could not be determined. For Gly26 and Gly29, only one of the two $C_\alpha H$ peaks (down-field shifted) is represented. The horizontal lines enclosing the range ±0.05 ppm represent the experimental error.

contains information on backbone–side chain and side chain–side chain interactions. Cross peaks away from the diagonal indicate interaction between residues that are located far from one another in the linear sequence but are close in space. Three regions are of interest: residues 8–10, 13–15, and 20–27. The presence of turns at Cys10–Lys11 or Lys11–Lys12, and Gly26–Tyr27, and a 3_{10}-helix at residues 13–15 have already been mentioned. Of significance are the observed cross peaks corresponding to $d_{\alpha\alpha}$ (9–27), $d_{N\alpha}$ (10–27), $d_{N\alpha}$ (29–10), d_{NN} (21–29), $d_{\alpha\alpha}$ (22–28), $d_{N\alpha}$ (23–28), $d_{N\alpha}$ (25–29), and $d_{N\alpha}$ (29–23). These findings support a triple-stranded β-sheet. At 700 ms, the following additional connectivities were found: d_{NN} (8–28), d_{NN} (10–28), d_{NN} (23–29), and d_{NN} (25–28), thus further supporting the presence of a triple-stranded β-sheet involving residues 8–10, 29–27, and 21–25. The pattern of NOE connectivities observed indicates an antiparallel β-sheet involving residues 8–10 and 27–29. Additional support for the presence of the above-mentioned secondary structural elements is provided by the slowed exchange rates observed for the amide hydrogens of Cys10, Ser14, Asp15, Cys16, Val21, Cys22, Leu23, Tyr27, Cys28, and Gly29 (Figure 5); these hydrogens exchange slowly in a time period of 4 h, whereas all other hydrogens exchange within 0.5 h. Seven of these backbone NH's, viz., those of Cys10, Asp15, Cys16, Val21, Leu23, Cys28, and Gly29, have been known to be involved in hydrogen-bonding interactions as available from the crystal structure data of CMTI-I (Bode et al., 1989). Presence of strong $d_{N\alpha}$ connectivities and lack of other NOE connectivities for residues other than those mentioned above (Figure 6) indicate that these residues are most likely in an extended conformation.

Discussion

Likos (1989) has reported the sequential proton assignments for CMTI-III at pH 2.8, 30 °C and identified a triple-stranded β-sheet as the secondary structural element made up of residues 8–10, 21–23, and 26–29. The CMTI-III* results reported here point out a similar triple-stranded β-sheet structure consisting of residues 8–10, 29–27, and 21–25. Heitz et al. (1989) have reported the solution conformation of *Ecballium elaterium* trypsin inhibitor II (ECTI-II), a member of the squash family. The secondary structure elements reported for this inhibitor include a mini-antiparallel β-sheet made up of residues 7–9 and 25–27, a β-hairpin made with residues 20–28 with a β-turn involving residues 22–25. Holak et al. (1989a) in reporting their NMR structure for CMTI-I assert that they find no evidence for the presence of a mini-antiparallel β-sheet which would involve residues 9–11 and 26–29. Our NOE results for CMTI-III* (Figure 6) indicate the presence of backbone–backbone interactions between residues 9 and 27, 10 and 27, and 10 and 29. With the additional NOE connectivities observed at 700 ms between residues 8 and 28, and 10 and 28, these results appear to support the presence of a

mini-antiparallel β-sheet involving residues 8–10 and 29–27.

Comparison of CMTI-III and CMTI-III.* In order to make a valid comparison of CMTI-III and CMTI-III* for identifying amino acid residues that are affected by hydrolysis of the Arg5–Ile6 peptide bond, we have made sequential proton resonance assignments for virgin CMTI-III at pH 4.71, 30 °C: Figure 7 shows a portion of the TOCSY contour map of CMTI-III in which the assignments are indicated. The sequence-specific assignments of CMTI-III, made by making use of DQF-COSY and NOESY data, are included in Table I. Because of the poor signal to noise ratio, chemical shift positions of cross peaks due to $C_\alpha H$'s Cys10, Lys12, and His25 could not be determined with certainty.

The chemical shifts of backbone NH and $C_\alpha H$ peaks are compared for CMTI-III and CMTI-III* in Figure 8 (panels A and B, respectively). The NH chemical shift differences (Figure 8A) indicate significant changes beyond the experimental error of ±0.05 ppm for residues near the reactive-site region, viz., Val2, Arg5, Leu7, Met8, and Lys9, and for residues near the C-terminal, viz., Leu17, Cys20, Leu23, His25, Cys28, and Gly29. Similarly, the $C_\alpha H$ chemical shift differences (Figure 8B) indicate that the N-terminal residues, viz., Cys3, Arg5, Ile6, Leu7, Met8, and Lys9 and the C-terminal residues, viz., Asp15, Cys20, Gly26, and Tyr27, undergo significant chemical shift changes. The largest shift change is observed for the NH of Arg5 (0.64 ppm). In addition, some side chains, especially those of Pro4, Arg5, Ile6, Leu7, and Leu23, show significant chemical shift changes upon modification of the reactive site in CMTI-III (Table I). These spin systems are identified in the TOCSY map shown in Figure 9A,B. Chemical shifts are sensitive probes of conformational changes, although by themselves they cannot be used to define a conformation (Pardi et al., 1983; Campbell et al., 1985). While it is not possible to determine atom displacement in terms of chemical shift differences, it is clear that hydrolysis of the Arg5–Ile6 peptide bond leads to larger tertiary structural changes for residues closer to the reactive site, and these perturbations are propagated throughout the molecule, including the C-terminal. It is of interest to note that while significant tertiary structural changes are indicated for CMTI-III*, its secondary structural elements, including the turn involving residues 8–12, remain unaffected by the cleavage of the peptide bond between Arg5 and Ile6. The X-ray crystallographic studies of CMTI-I in complex with trypsin indicate that, among the residues whose chemical shifts are affected by the reactive-site peptide bond hydrolysis, Met8, Cys16, Leu17, Val21, Leu23, Cys28, and Gly29 are involved in hydrogen-bonding interactions (Bode et al., 1989). The hydrogen-bonding interactions are apparently not significantly affected by the reactive-site hydrolysis, as evidenced by absence of significant changes in the slowed exchange rates of amide hydrogens of these residues (Figure 5). Residues Arg1–Leu7 and Glu9 make 131 intermolecular contacts and residues His25–Gly29 make 7 intermolecular contacts in the trypsin–inhibitor complex, as revealed by X-ray crystallography (Bode et al., 1989). Thus, one might expect changes in these interactions based on our NMR results. Indeed, the equilibrium dissociation constants for the enzyme–inhibitor complexes formed by virgin and modified CMTI-III with trypsin have been found to be 2.4×10^{-8} M and 2.2×10^{-9} M, respectively (Krishnamoorthi et al., 1990). Furthermore, CMTI-III* and CMTI-I* do not inhibit activated Hageman factor, a serine proteinase involved in blood coagulation, whereas the virgin inhibitors do (Hojima et al., 1982; Krishnamoorthi et al., 1990). Thus, the loss of the inhibitor's activity toward Factor XII_a is due to the conformational changes undergone by a few

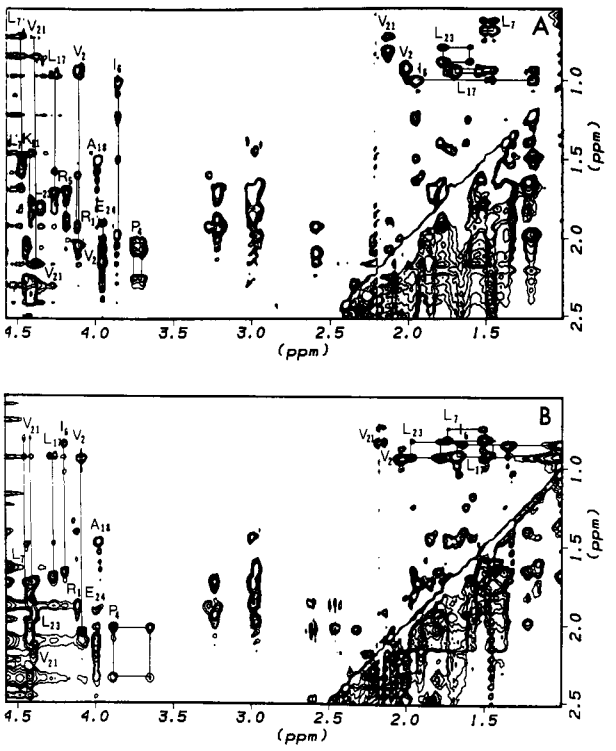

FIGURE 9: Comparison of portions of TOCSY maps of virgin and modified CMTI-III in H_2O, pH 4.71, 30 °C: (A) CMTI-III*; (B) CMTI-III. Side chains of residues Pro4, Arg5, Ile6, Leu7, and Leu23 which show significant chemical shift changes upon hydrolysis of the Arg5–Ile6 peptide bond are identified.

functional residues that come into contact with the enzyme in the inhibitor–enzyme complex. In the following paper (Krishnamoorthi et al., 1992), we provide evidence for the conformational changes introduced by the hydrolysis of the reactive-site peptide bond by measuring the ionization behavior of a side chain located at a distance from the reactive-site region, namely, the pK_a of His25, which indeed changes by 0.24 unit (5.47 in CMTI-III and 5.71 in CMTI-III*).

Comparison of CMTI-I and CMTI-III. Chemical shifts of backbone hydrogens, NH's, and $C_\alpha H$'s, of CMTI-I and CMTI-III are compared in panels C and D, respectively, of Figure 8. The two proteins differ by a single residue substitution: CMTI-III has a Lys at position 9 instead of a Glu as in CMTI-I (Wieczorek et al., 1985). The NMR data of CMTI-I, taken from the work of Holak et al. (1989a), correspond to the condition of pH 4.31, 25 °C. The results indicate that this single drastic substitution of an acidic amino acid residue by a basic one causes small, but definite, changes in the backbone hydrogen chemical shifts of residues 8, 9, 15–17, 20, 22, and 29. Compared with the backbone chemical shift changes observed for the modification of the reactive site, these changes are small (<0.15 ppm). Temperature dependencies of the backbone NH chemical shifts of CMTI-I* (Krishnamoorthi et al., unpublished results) in the range 10–45 °C indicate changes within experimental error for all the residues for 5 °C; the CαH chemical shifts are temperature-independent. The solution structure of CMTI-I (Holak et al., 1989a) shows that the side chain of Glu is exposed to the solvent and is not involved in any interaction with other side chains. The residues that show chemical shift changes due the substitution Lys9/Glu are predominantly those that form the secondary structural elements; residues 8–10 and 29–27 form the two turns, residues 13–16 form a 3_{10}-helix, and residues 21–25 are involved the formation of a triple-stranded β-sheet. The residues that are in an extended conformation

are apparently not affected significantly. One of the conformational consequences of the above substitution is demonstrated by the ionization property of His25, whose pK_a is 5.72 ± 0.02 in CMTI-I and 5.47 ± 0.02 in CMTI-III (Krishnamoorthi et al., 1992). Furthermore, the association equilibrium constants determined for the binding of CMTI-I and CMTI-III to activated Hageman factor (Wynn & Laskowski, 1990) indicate that the value for CMTI-III is about 62 times that for CMTI-I. However, the dissociation equilibrium constants determined for the trypsin–CMTI-I and trypsin–CMTI-III complexes do not reveal any significant differences in stability (1.7×10^{-8}M and 2.4×10^{-8}M, respectively; Krishnamoorthi et al., 1990). In order to describe completely the tertiary structural changes, as reflected by chemical shift changes, studies involving distance-geometry algorithm and NOESY data (Havel & Wüthrich, 1985; Braun, 1987) will be carried out on CMTI-III and CMTI-III*.

Conclusions. Hydrolysis of the Arg5–Ile6 peptide bond in CMTI-III causes significant chemical shift changes to residues located not only close to, but also far from, the reactive site, indicating tertiary structural changes that are transmitted throughout the molecule. The secondary structural elements are, however, not affected. The drastic substitution of Glu9 in CMTI-I by a Lys in CMTI-III leads to relatively smaller chemical shift changes for a few residues located near and away from the site of substitution. Residues whose chemical shifts are affected make up the secondary structural elements of the protein molecule; residues that are in an extended conformation are not affected.

ACKNOWLEDGMENTS

We acknowledge helpful comments from the anonymous referees. This is publication 91-440-J of the Kansas Agricultural Experiment Station.

SUPPLEMENTARY MATERIAL AVAILABLE

Complete listing of observed NOEs and the assigned NOESY contour map of CMTI-III* (3 pages). Ordering information is given on any current masthead page.

REFERENCES

Anil Kumar, Ernst, R. R., & Wüthrich, K. (1980) *Biochem. Biophys. Res. Commun. 95*, 1–6.

Bax, A. (1989) *Annu. Rev. Biochem. 58*, 223–256.

Bax, A., & Davis, D. G. (1985) *J. Magn. Reson. 65*, 355–360.

Billeter, M., Braun, W., & Wüthrich, K. (1982) *J. Mol. Biol. 155*, 321–346.

Bode, W., Greyling, H. J., Huber, R., Otlewski, J., & Wilusz, T. (1989) *FEBS Lett. 242*, 285–292.

Braun, W. (1987) *Q. Rev. Biophys. 19*, 115–157.

Braunschweiler, L., & Ernst, R. R. (1983) *J. Magn. Reson. 53*, 521.

Campbell, I. D., Dobson, C. M., & Williams, R. J. P. (1985) *Biochem. J. 231*, 1–10.

Havel, T. F., & Wüthrich, K. (1985) *J. Mol. Biol. 182*, 281–294.

Hojima, Y., Pierce, J. V., & Pisano, J. J. (1982) *Biochemistry 21*, 3741–3746.

Holak, T. A., Gondol, D., Otlewski, J., & Wilusz, T. (1989a) *J. Mol. Biol. 210*, 635–648.

Holak, T. A., Bode, W., Huber, R., Otlewski, J., & Wilusz, T. (1989b) *J. Mol. Biol. 210*, 649–654.

Heitz, A., Chiche, L., Le-Nguyen, D., & Castro, B. (1989) *Biochemistry 28*, 2392–2398.

Krishnamoorthi, R., Gong, Y., & Richardson, M. (1990) *FEBS Lett. 273*, 163–167.

Krishnamoorthi, R., Lin, C. S., Gong, Y., VanderVelde, D., & Hahn, K. (1992) *Biochemistry* (following paper in this issue).

Kupryszewski, G., Ragnarsson, U., Rolka, K., & Wilusz, T. (1986) *Int. J. Pept. Protein Res. 27*, 245–250.

Laskowski, M., Jr., & Kato, I. (1980) *Annu. Rev. Biochem. 49*, 593–626.

Likos, J. J. (1989) *Int. J. Pept. Protein Res. 34*, 381–386.

Marion, D., & Wüthrich, K. (1983) *Biochem. Biophys. Res. Commun. 113*, 967–974.

McWherter, C. A., Walkenhorst, W. F., Campbell, E. J., & Glover, G. I. (1989) *Biochemistry 28*, 5708–5714.

Otlewski, J. (1990) *Biol. Chem. Hoppe-Seyler 371 Suppl.*, 23–28.

Pardi, A., Wagner, G., & Wüthrich, K. (1983) *Eur. J. Biochem. 137*, 445–454.

Piantini, U., Sorensen, O. W., & Ernst, R. R. (1982) *J. Am. Chem. Soc. 104*, 6800–6801.

Rance, M., Sorensen, O. W., Bodenhausen, G., Wagner, G., Ernst, R. R., & Wüthrich, K. (1983) *Biochem. Biophys. Res. Commun. 117*, 479–485.

Wieczorek, M., Otlewski, J., Cook, J., Parks, K., Leluk, J., Wilimowska-pelc, A., Polanowski, A., Wilusz, T., & Laskowski, M., Jr. (1985) *Biochem. Biophys. Res. Commun. 126*, 646–652.

Wüthrich, K. (1986) *NMR of Proteins and Nucleic Acids*, pp 1–292, Wiley, New York.

Wüthrich, K., Wider, G., Wagner, G., & Braun, W. (1982) *J. Mol. Biol. 155*, 311–319.

Wynn, R., & Laskowski, M., Jr. (1990) *Biochem. Biophys. Res. Commun. 166*, 1406–1410.